Desalination and Water Treatment
www.deswater.com
doi: 10.1080/19443994.2013.870062

53 (2015) 2970–2979
March

Taylor & Francis
Taylor & Francis Group

Decolorization of rhodamine B using hydrogen peroxide and $H_3PW_{12}O_{40}$@C photocatalyst synthesized *in situ* under ultraviolet irradiation

Changchao Zhan[a,b,*], Mingqiang Zhong[a,*], Feng Chen[a], Jintao Yang[a], Xiaohua Cao[a,b], Xiaoping Jiang[a,b]

[a]*College of Chemical Engineering and Materials, Zhejiang University of Technology, Hangzhou 310014, China*
Tel./Fax: +86 571 88320856; emails: zhan223@163.com (C. Zhan); zhongmq@zjut.edu.cn (M. Zhong)
[b]*College of Chemistry and Environmental Engineering, Jiujiang University, Jiujiang 332005, China*

Received 9 June 2013; Accepted 21 November 2013

ABSTRACT

The $H_3PW_{12}O_{40}$@C photocatalysts synthesized *in situ* from dodetungstophosphoric acid (TPA) and soluble starch were studied and characterized by FTIR, XRD, scanning electron microscope, and energy dispersive X-ray analysis. The degradation of rhodamine B (RhB) wastewater with $H_3PW_{12}O_{40}$@C photocatalysts and hydrogen peroxide was investigated under ultraviolet irradiation. The effect of different factors and synergetic effect on the degradation of RhB were studied and the mechanism of catalytic oxidation of RhB was discussed. The results showed that the RhB was degraded efficiently. The decoloration efficiency of the RhB was up to 94.6% with initial pH value of 6 and RhB concentration of 100 mg/L under better reaction conditions (i.e. hydrogen peroxide concentration of 12 mM, PW30 (represented raw materials formula according to weight ratio of TPA to soluble starch is 30%) mass of 1.0 g/L, reaction temperature of 25°C, the high pressure mercury lamp power of 500 W, and the radiation time of 70 min). Degradation process of RhB wastewater by ultraviolet, hydrogen peroxide, and PW30 has synergetic effect.

Keywords: Ultraviolet; $H_3PW_{12}O_{40}$@C photocatalysts; H_2O_2; Decolorization; Rhodamin B

1. Introduction

The textile industry wastewater is often difficult to degrade because it contains complex organic molecules, like dyes [1,2]. Most dyes are toxic and recalcitrant to biodegradation, causing a decay in the efficiency of biological plants currently used for the treatment of wastewaters containing such compounds [3,4]. To fight this problem, advanced oxidation processes (AOPs) such as homogeneous and heterogeneous photocatalysis are promising technologies, which can be useful for achieving total decolorization with partial degradation of some dyes in waters [5–7].

AOPs refer to a set of different methods leading to the generation of highly oxidative species such as hydroxyl radicals ($^{\bullet}OH$) which are powerful oxidizing agents that are able to mineralize biorecalcitrant organics in the effluents or at least convert them to easily biodegradable compounds [8]. A UV/H_2O_2 process can be carried out under ambient conditions and

*Corresponding authors.

can lead to complete mineralization of organic carbon to CO_2 and H_2O [9–12]. A heterogeneous oxidation process employing hydrogen peroxide and photocatalyst with UV light has been found to be a highly efficient AOP in the decolorization and mineralization of wastewaters containing various organic compounds [13–15].

The Keggin heteropolyacids (HPAs) such as 12-tungstophosphoric acid, can catalytically activate hydrogen peroxide and be considered soluble models of semiconductor, which is an environmentally friendly and inexpensive oxidant and photocatalyst [16,17]. However, a major drawback to the HPAs system is its high water solubility, which impedes recovery and reuse of the catalyst. To conquer this shortcoming, several studies have put efforts into the immobilization of the HPAs on high-surface-area solid supports, such as carbon gel, activated carbon, ZrO_2, and SiO_2 as heterogeneous catalysts [18–20].

The main objectives of this work were (1) to demonstrate the treatment efficiency of rhodamine B (RhB) using ultraviolet in the presence of $H_3PW_{12}O_{40}$@C–H_2O_2 process; (2) to investigate the effects of several experimental parameters including loading of $H_3PW_{12}O_{40}$, pH value, dosage of $H_3PW_{12}O_{40}$@C, H_2O_2 concentration, and reuse on decolorization efficency; and (3) to explore the possible mechanism of RhB decolorization based on the observed experimental results.

2. Experimental

2.1. Materials

Soluble starch, $H_3PW_{12}O_{40}\cdot 6H_2O$ (abbreviated as PW12), RhB, hydrogen peroxide solution (30%), and other compounds such as HCl, NaOH were purchased from Sinopharm Chemical Reagent Co. Ltd (China). Solutions were prepared by dissolving the requisite quantity of the dye in deionized water. Chemical structure of RhB is given in Fig. 1.

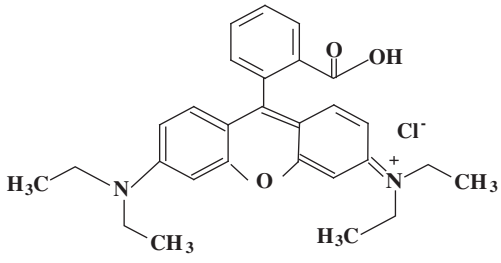

Fig. 1. Molecular structure of RhB.

2.2. Preparation of the $H_3PW_{12}O_{40}$@C photocatalysts

The soluble starch and $H_3PW_{12}O_{40}\cdot 6H_2O$ were used as received. A desired amount of soluble starch was added to 25 mL of deioned water containing a certain amount of PW12 and then the mixture was stirred for 2 h at 55–60℃. The dark colour $H_3PW_{12}O_{40}$@C photocatalysts were obtained (Fig. 5(a)) after calcination at 200℃ for 10 h using a conventional oven under air atmosphere and grounded into 150 mesh grains in sequence, which were denoted as PW10, PW30, PW50 according to the weight ratio of PW12 to soluble starch, respectively. The possible formation mechanism of $H_3PW_{12}O_{40}$@C photocatalysts was figured out as Fig. 2 [21].

2.3. Apparatus and analysis

UV-2501PC (Shimadzu, Japan) UV-vis spectrometer was used to determine the dye concentrations (λ_{max} = 553 nm). The percentage of dye decolorization efficiencies were calculated by using the following Eq. (1):

$$\text{Percentage decolorization efficiency} = (1 - C_t/C_0) \times 100 \quad (1)$$

where C_0 is the initial dye concentration, C_t is the dye concentration at measurable time t.

The degradation of RhB dye was confirmed by Agilent1200LC high pressure liquid chromatography (HPLC) equipped with UV-vis diode array detector using Agilent XDB-C_{18} column (150 × 4.6 mm) in the reverse phase mode. The HPLC separation was carried out using mixed eluent (CH_3OH:H_2O = 3:1 by volume, λ = 550 nm) at a flow rate of 1 mL/min. The column temperature was 30℃, with an injection volume of 20 μL.

The PW30 particles as prepared and after five cycles of uses in ultraviolet/PW30@C-H_2O_2 system were photographed by scanning electron microscope (SEM) (TESCAN-Vega II, operating at a voltage of 30 kV) to demonstrate the different pore structure characteristics. Energy dispersive X-ray spectrum analysis was investigated by an energy dispersive X-ray spectrometer EDX Oxford INCA X-act. XRD measurements were performed on a Germany Bruker-D8 Advance X-ray diffractometer, with graphite-monochromatized high-intensity Cu-Kα radiation at 40 kV and 30 mA. The IR spectrum of the $H_3PW_{12}O_{40}$@C particles was recorded on FTIR spectrometer (M-1370, Perkin-Elmer Company, USA).

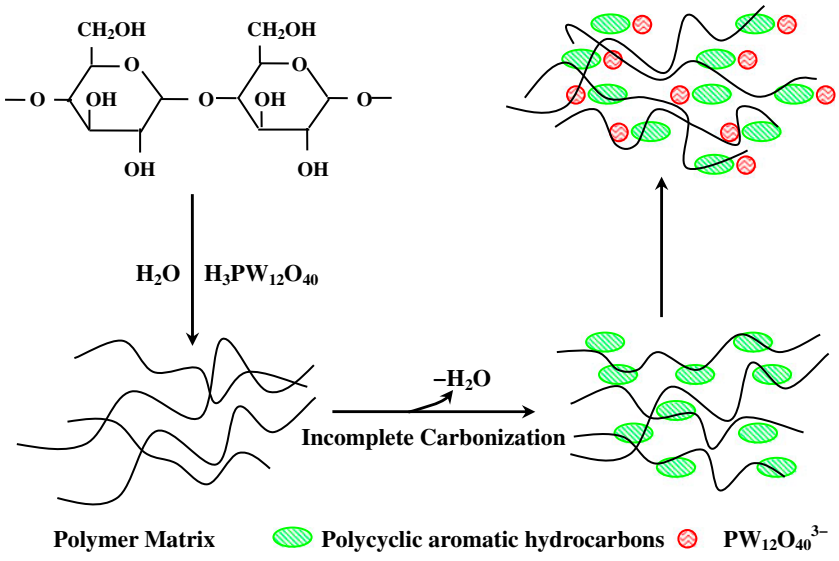

Fig. 2. Formation mechanism of $H_3PW_{12}O_{40}$@C photocatalysts.

2.4. General procedure

In a 500 mL beaker with jacket which was surrounded by circulated water to be kept at the needed temperature, aqueous solution of dye (250 mL), hydrogen peroxide, and $H_3PW_{12}O_{40}$@C or PW12 were added. The mixture was irradiated under the ultraviolet irradiation at a set temperature for a period. A 500 W mercury bulb (Institute of Electrical Light Source, Beijing, China) was used as UV irradiation source and were positioned over RhB solution at the height of 20 cm. After the suspension was irradiated for a certain time, 5 mL suspension was taken out and centrifugalized, then the RhB concentration of clean solution was measured.

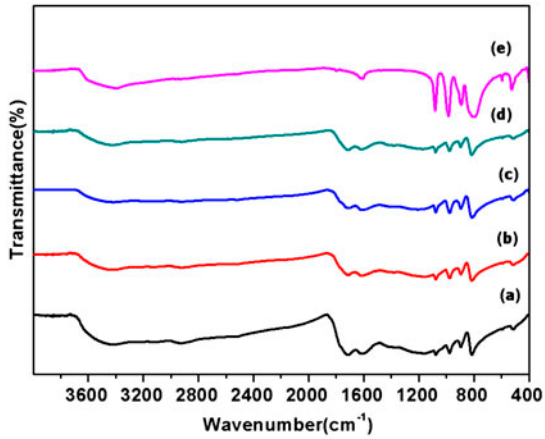

Fig. 3. IR spectra of (a) PW10, (b) PW30, (c) PW50, (d) PW30 after five cycles of uses in ultraviolet/ $H_3PW_{12}O_{40}$ @C–H_2O_2, and (e) PW12.

3. Results and discussion

3.1. Characterization of $H_3PW_{12}O_{40}$ @C photocatalysts

3.1.1. Infrared spectrum

The Fourier transform infrared spectrum of photocatalysts calcination (Fig. 3(a)–(d)) at 200 ℃ showed that the species present were the undegraded $[PW_{12}O_{40}]^{3-}$ anion. Corresponding to the earlier reported data, the IR spectrum of $H_3PW_{12}O_{40}$ has four strong bands at 1,080, 981, 890, and 805 cm^{-1}, which are designated to the stretching vibrations of P–O, W = O_t, W–O_c–W, and W–O_e–W, respectively [18,22–24]. The broad absorption band around 3,420 cm^{-1} (the ν (OH) vibration) and the peak at 1,614 cm^{-1} (ν (H_2O)) indicate that the solid HPW accommodates a large amount of water of crystallization as well as the H^+. The peaks appearing at 1,720, 1,630, 592, and 515 cm^{-1} are assigned to the vibration of ν (C=O), ν (C=C), δ(O–P–O), and ν (W–O–W), respectively. This indicates that PW30 (Fig. 3(d)) still kept typical Kiggen structure after five times of uses in ultraviolet/PW30-H_2O_2 process.

3.1.2. X-ray diffraction patterns

X-ray diffraction patterns of $H_3PW_{12}O_{40}$@C photocatalysts (Fig. 4(a)–(c)) showed the same diffraction

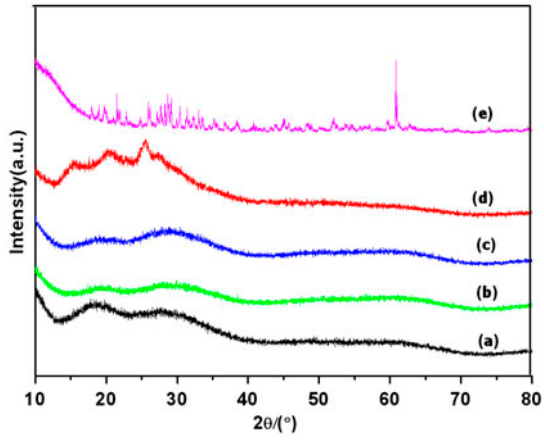

Fig. 4. XRD patterns of (a) PW10, (b) PW30, (c) PW50, (d) PW30 after five cycles of uses in ultraviolet/ $H_3PW_{12}O_{40}$@C–H_2O_2, and (e) PW12.

patterns, possibly owing to a high dispersion of non-crystalline species. In the above $H_3PW_{12}O_{40}$@C composites, acid–base interaction but not physical adsorption existed between PW12 molecule and the carbon support [25,26]. That is, chemically active surface hydroxyl groups(–C–OH) of soluble starch were protonated in an acidic medium to form $-C-OH_2^+$ groups, the process is described in Eq. (2):

$$-C-OH + H^+ = -C-OH_2^+ \quad (2)$$

The $-C-OH_2^+$ group should act as a counter ion for $H_2PW_{12}O_{40}^-$ ion and yielded $(-C-OH_2^+)(H_2PW_{12}O_{40}^-)$ composite by acid–base reaction. On the other hand, hydrogen bondings such as $W=O_t\cdots HO-C$, $W-O_c\cdots HO-C$, $W-O_e\cdots HO-C$ also existed in the composites. The above two kinds of the interactions ensure little leakage of the PW30 from the carbon support during subsequent photocatalysis tests.

In addition, the sharp reflection peak at $2\theta = 25.6^\circ$ appears in PW30 (Fig. 4(d)) after five cycles of uses in ultraviolet/ PW30-H_2O_2, which suggests that the carbon crystallinity of PW30 is promoted further by catalytic oxidation reaction compared with PW30 (Fig. 4(b)) [27].

3.1.3. SEM and EDX

SEM analysis showed that all the samples consisted of agglomerates of particles with the diameters from about 10–100 μm. The SEM image of PW12 (Fig. 5(a)) shows spherical particles with an average size of approximately 10 μm. SEM surfaces of PW30 particles after five cycles of uses in ultraviolet/PW30-H_2O_2 (Fig. 5(c)) reveals that very few surfaces of PW30 with ultraviolet irradiation show patterns of crevice-like pores and become rough compared with the fresh PW30 photocatalysts (Fig. 5(b)).

Quantitative elemental EDX analyses of a group of the samples were carried out with spatially resolved EDX spectrum (see to Fig. 6). EDX analysis of PW30 after five cycles of uses reveal that tungsten content has slightly decreased compared with PW30, which is consisted with EDX data of PW30 and PW30 after five cycles of uses. EDX results show that the main composition elements in all photocatalysts supported on carbon are C, O, P, and W (Table 1).

3.2. Effect of PW12 loading dosage on decolorization efficiency of RhB

The effect of PW12 loading dosage on decolorization efficiency of RhB was investigated with photocatalyst concentration of $0.4\,g\,L^{-1}$. Photocatalysts of PW10, PW30, and PW50 represented the synthesis raw materials weight ratio of PW12 to soluble starch is 10, 30, and 50%, respectively. The results are shown

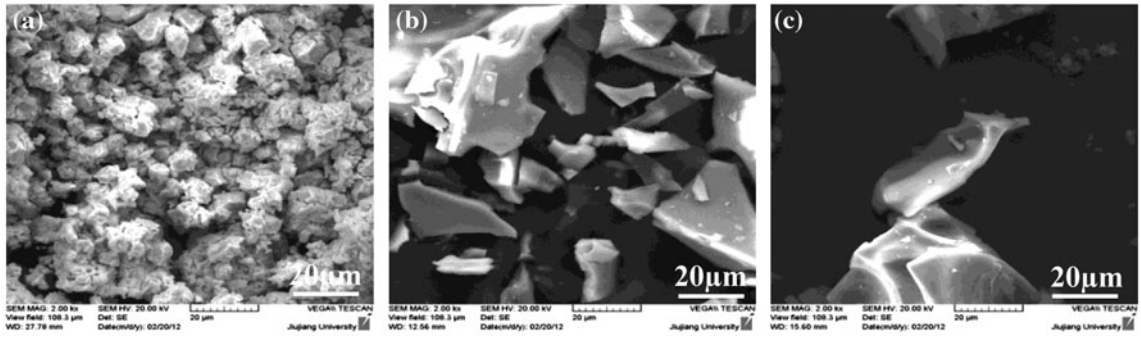

Fig. 5. SEM micrographs of photocatalysts: (a) PW12, (b) PW30, and (c) PW30 after five cycles of uses in ultraviolet/ $H_3PW_{12}O_{40}$@C–H_2O_2.

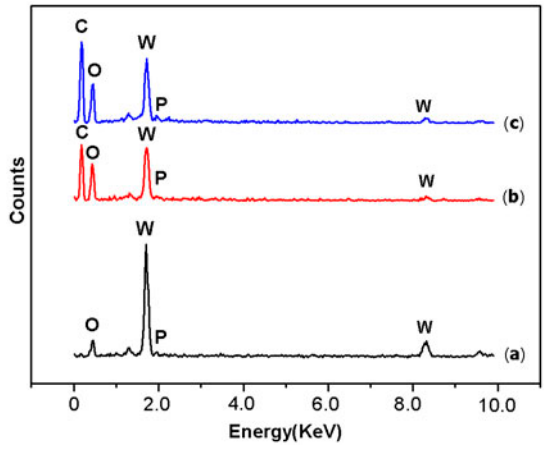

Fig. 6. The EDX spectra of (a) PW12, (b) PW30, and (c) PW30 after five cycles of uses.

Table 1
Data of EDX for PW12, PW10, PW30, PW50, and PW30 after five cycles of uses

	Content (wt %)				
Elements	PW12 (a)	PW10	PW30 (b)	PW30 used after five times (c)	PW50
C	Blank	72.42	40.57	46.32	19.72
O	18.47	16.21	33.34	30.45	44.26
W	79.87	11.26	25.83	22.99	35.61
P	1.66	0.11	0.26	0.24	0.41

in Fig. 7. The decolorization efficiency increases when the PW12 loading dosage ranging from 10% to 30% and decolorization efficiency have little decrease when the PW12 loading dosage is 50%. Furthermore, decolorization efficiency was 27.5% with the same mass of PW12 as neat photocatalyst at 70 min, which indicates that the PW12 supported on a suitable carbon carrier can obtain higher photocatalytic activity. The increasing of decolorization efficiency is originated from surface structure of the $H_3PW_{12}O_{40}$@C, which coupled photogenerated carrier's ability of PW12 with dispersion and adsorption of carbon with larger specific surface area. However, excessive loading dosage resulted in decrease of photocatalytic activity due to accumulation of PW12 on the surface of carbon supports.

3.3. Effect of pH on decolorization efficiency of RhB

The ultraviolet decolorization efficiency of RhB in the presence of PW30-H_2O_2 was investigated at pH = 2–10. The results are shown in Fig. 8. When the reaction time was 70 min, the decolorization effciencies are 69.3% (pH = 2), 62.6% (pH = 4), 62.3% (pH = 6), 39.3% (pH = 8), and 54.3% (pH = 10), respectively. From the results, we can find that RhB readily decomposed by the ultraviolet/PW30-H_2O_2 process in the range of initial pH between 2 and 6. The decolorization efficiency of RhB at low pH is better than that at higher pH. It is possible that the change in the solution pH results in the change of hydrophobic property of the dye and impact on generation rules of hydroxyl radicals, which affects the ultraviolet decolorization. In addition, the presence of large quantities of OH^- ions in the

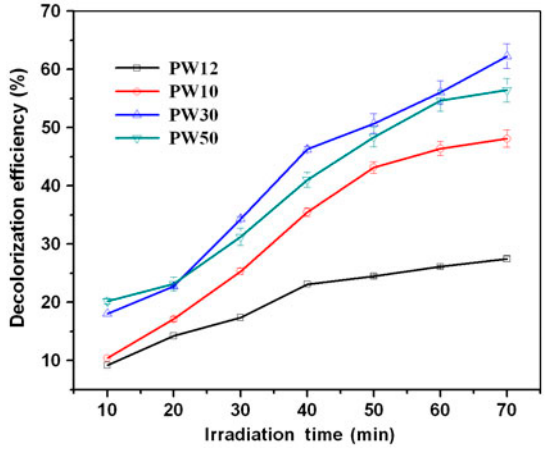

Fig. 7. Effect of PW12 loading dosage on RhB decolorization efficiency.
Conditions: initial pH = 6, [RhB] = 100 mg L^{-1}, [H_2O_2] = 2 mM, temperature = 25°C, time = 70 min, photocatalyst concentration = 0.4 g L^{-1}.

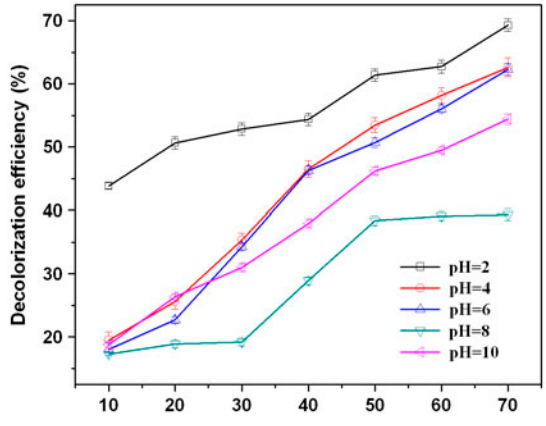

Fig. 8. Effect of solution pH on RhB decolorization efficiency.
Conditions: initial pH = 2–10, [RhB] = 100 mg L^{-1}, [H_2O_2] = 2 mM, temperature = 25°C, time = 70 min, PW30 concentration = 0.4 g L^{-1}.

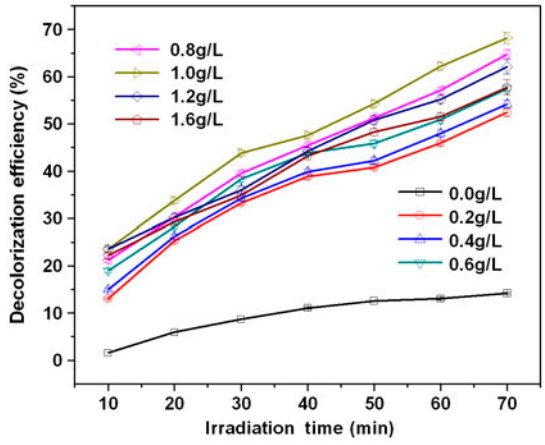

Fig. 9. Effect of PW30 dosage on RhB decolorization efficiency.
Conditions: initial pH = 6, [RhB] = 100 mg L^{-1}, [H_2O_2] = 2 mM, PW30 concentration = 0–1.6 g L^{-1}, temperature = 25°C, time = 70 min.

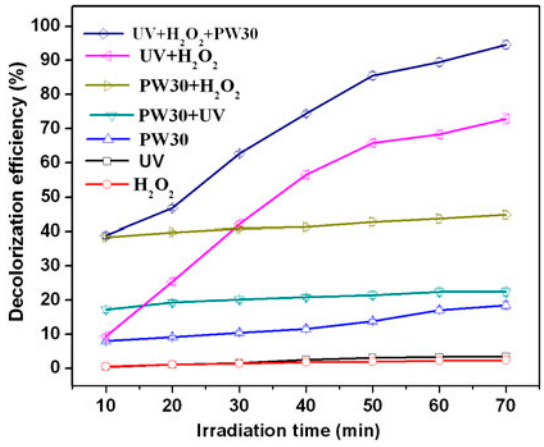

Fig. 11. The decolorization efficiency of RhB in different reaction systems.
Conditions: initial pH = 6, [RhB] = 100 mg L^{-1}, [H_2O_2] = 12 mM, temperature = 25°C, time = 70 min, PW30 concentration = 1 g L^{-1}.

reaction medium favors the formation of $OH^{\bullet}$ radical, which is widely accepted as principal oxidizing species responsible for decolorization process at neutral or high pH levels and results in higher decolorization efficiency at pH = 10 than that of at pH = 8 [28].

3.4. Effect of PW30@C dosage on decolorization efficiency of RhB

The effect of PW30 dosage ranging from 0.0 to 1.6 g L^{-1} on the ultraviolet decolorization efficiency of RhB was investigated. The results are shown in Fig. 9.

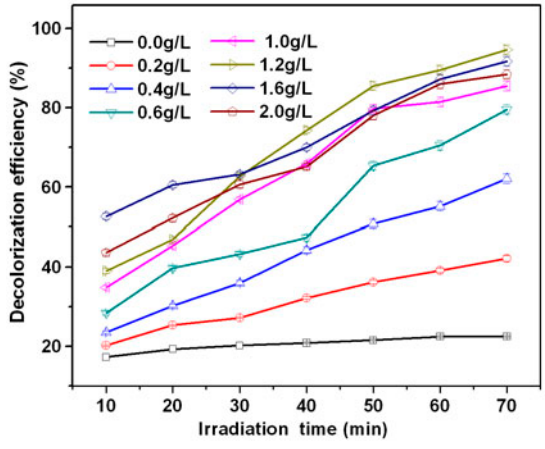

Fig. 10. Effect of hydrogen peroxide dosage on RhB decolorization efficiency.
Conditions: initial pH = 6, [RhB] = 100 mg L^{-1}, [H_2O_2] = 0–20 mM, temperature = 25°C, time = 70 min, PW30 concentration = 1 g L^{-1}.

From this we can see that keeping H_2O_2 concentration constant (2 mM), the decolorization effciencies of dye solutions increased with the PW30 dosage, but as the PW30 dosage exceeds 1.0 g/L, the decolorization efficiency increased very slowly. With a consequent increase in dosage of PW30 ultraviolet light transmission rate should decrease, which is unfavorable to catalyze the holysis of H_2O_2. This would be suffcient to explain decolorization effciencies of RhB aqueous solutions kept at constant level.

3.5. Effect of hydrogen peroxide concentration on decolorization efficiency of RhB

The effect of the initial concentration of H_2O_2 on ultraviolet decolorization of RhB was investigated. The

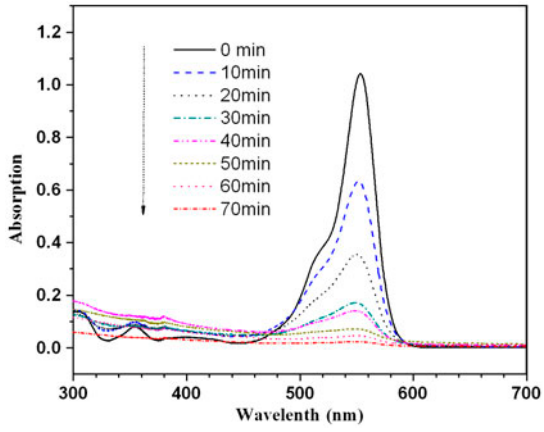

Fig. 12. UV-vis spectra of RhB under better reaction conditions.

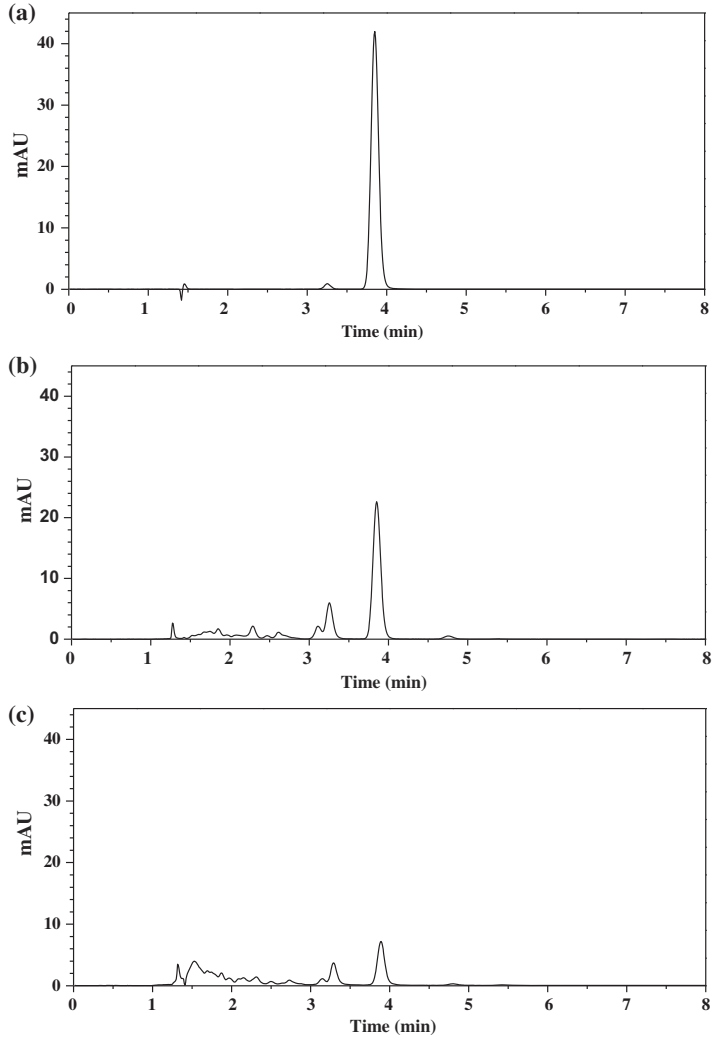

Fig. 13. HPLC chromatogram of degraded samples at different time intervals (a) 0 min, (b) 30 min, and (c) 70 min.

results are shown in Fig. 10. By increasing the H_2O_2 initial concentration, the oxidative ability of the system was promoted. The decolorization effiencies of dye solutions were increased. When hydrogen peroxide concentration exceeds 12 mM, the decolorization efficiency increased very slowly with further increase of the hydrogen peroxide concentration. It is because that at high concentrations, the solution undergoes self quenching of $^{\bullet}OH$ radicals by added amounts of H_2O_2 to produce $HO_2^{\bullet}$ radicals [29].

$$H_2O_2 + {}^{\bullet}OH \longrightarrow H_2O + HO_2^{\bullet} \quad (3)$$

The peroxy radicals produced as a result of the follow reaction can also enter in other reaction pathways.

$$HO_2^{\bullet} + {}^{\bullet}OH \longrightarrow H_2O + O_2 \quad (4)$$

It is suggest that H_2O_2 is ineffectively decomposed so that decoloration effciencies of dye was not proportional to H_2O_2 dosage in this case.

3.6. Effect of ultraviolet coupled with PW30-H_2O_2

The decolorization of RhB aqueous solution in PW30/H_2O_2/ultraviolet, PW30/ultraviolet, PW30/H_2O_2, ultraviolet/H_2O_2, PW30, H_2O_2, ultraviolet was compared in Fig. 11. According to the Fig. 11, no decolorization almost occurred in ultraviolet or H_2O_2 systems. In PW30, ultraviolet/PW30, PW30-H_2O_2, ultraviolet-H_2O_2 and ultraviolet/PW30-H_2O_2 systems, the decolorization efficiency was 18.5, 22.5, 44.8, 72.9, and 94.6%, respectively. It is obvious that the ultraviolet treatment in combination with

PW30-H_2O_2 showed a synergistic effect for RhB decolorization.

The UV-vis spectra are also useful to monitor the photodegradation process of organic pollutant. Therefore, the decolorization efficiency of RhB is characterized by UV-vis and the result is shown in Fig. 12. As can be seen from this figure, RhB shows two main strong absorption band at 553 and 350 nm, which should be attributed to the $n \rightarrow \pi^*$ electron transition and benzene ring structure of RhB, respectively. The absorbing peak of RhB at 553 nm became weaker and nearly disappeared after 70 min, which indicated that the chromophore and conjugated π systems were destroyed. The results are in good agreement with literature reported previously [30].

Photodegradation of RhB was further confirmed by the HPLC analysis of degraded samples. HPLC chromatogram of 0, 30, and 70 min are shown in Fig. 13(a)–(c). It was observed that the intensity of RhB peak decreases but the intensity of intermediate peaks at the retention time of 2.28, 1.74, and 1.27 min increase after 70 min photocatalytic degradation reaction. These results were similar to previous literatures reported [31,32].

3.7. Discussion of possible mechanism of RhB decolorization efficiency

The decoloration efficiency of the dye solution is mainly due to the reaction of hydroxyl radicals which generated from main two pathways (1) hydrogen peroxide in solution upon irradiation by ultraviolet [9–12].

$$H_2O_2 + h\nu \longrightarrow 2\ {}^{\bullet}OH \quad (5)$$

(2) It is clear that $H_3PW_{12}O_{40}$@C has a positive effect on catalytic decomposition of H_2O_2 when compared to decolorization efficiency of $H_3PW_{12}O_{40}$@C/H_2O_2 and H_2O_2 system in Fig. 11. So, reaction mechanism of photoexcited $H_3PW_{12}O_{40}$ in Fig. 14 has been suggested to take place during the reaction.

Excitation of $PW_{12}O_{40}^{3-}$ leads to an oxygen to metal [O^{2-}–W^{6+}] charge transfer excited state $H_3PW_{12}O_{40}^{*}$ in analogy to the photoinduced charge separation processes that occur in TiO_2 under ultraviolet ($\lambda <$ 400 nm). Then, $H_3PW_{12}O_{40}^{*}$ can abstract an electron from reductants (e.g. H_2O, H_2O_2) and hold the electron to form ${}^{\bullet}OH$ and $H_3PW_{12}O_{40}^{-}$ (reducing state). At last stage, O_2 can regenerate the starting $H_3PW_{12}O_{40}$ with parallel formation of ${}^{\bullet}O_2^{-}$ [16,33,34].

Since hydroxyl radicals and superoxygen anion are very strong oxidizing reagents, they can react with the dye molecules to produce intermediates which can cause the decoloration of the original solution:

$$ {}^{\bullet}OH + RH \longrightarrow P \quad (6)$$

$$ {}^{\bullet}O_2^{-} + RH \longrightarrow P \quad (7)$$

3.8. Reuse of PW30 photocatalyst

The stability of the photocatalyst is very important for its application in environmental manipulation. Therefore, the reuse of PW30 was examined for the degradation of RhB, during five cycle experiments. Each experiment was carried out under better reaction conditions.

The PW30 photocatalyst can be recycled with little leaching and loss in photoactivity (Fig. 15), which is consistent with infrared spectrum and EDX spectrum

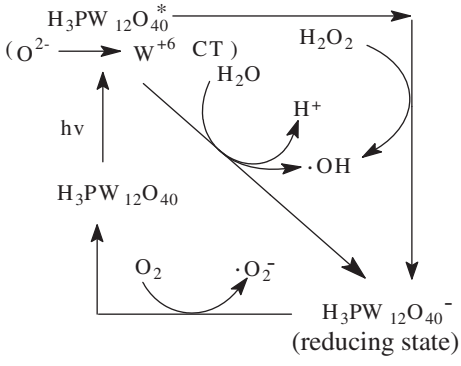

Fig. 14. Proposed reaction mechanism of photoexcited $H_3PW_{12}O_{40}$@C.

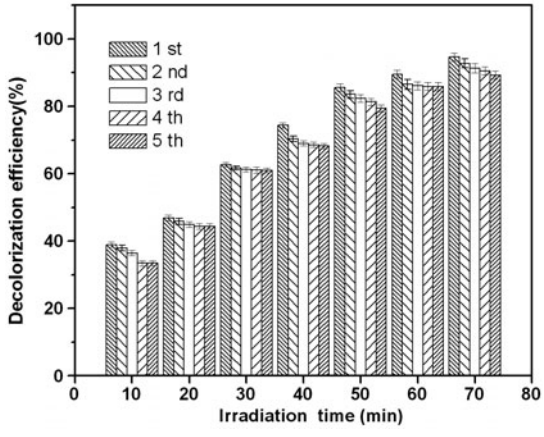

Fig. 15. The effect of reuse on decolorization efficiency of RhB by ultraviolet/PW30-H_2O_2.

of PW30 photocatalysts (Fig. 6(b) and (c)). PW30 showed good endurance of five cycles for 100 mg/L RhB solution degradation under UV irradiation in which decolorization efficiency also reached 89.3% without any deal.

4. Conclusion

The UV/PW30-H_2O_2 process seems to be a powerful method for decolorization of RhB, in which the carbon support provides a microenvironment for PW12, H_2O_2 that greatly enhances the photoreactivity of PW12. The decolorization efficiency was sensitive to operational parameters. The better process conditions involved in pH 6.0, PW (1.0 g/L), RhB concentration of 100 mg/L, hydrogen peroxide concentration of 12 mM, ultraviolet irradiation with 500 W power, temperature of 25°C, and reaction time for 70 min. Under better reaction conditions, the decolorization efficiency was 94.6%. Based on the proposed competitive mechanism for the H_2O_2 reactions in the presence of PW30, it can be concluded that the ultraviolet treatment in combination with PW30-H_2O_2 showed a synergistic effect for RhB decolorization, the photoinduced charge separation processes that occur in $H_3PW_{12}O_{40}$@C under ultraviolet can also promote the decomposition of H_2O_2.

Acknowledgment

We thank the National Natural Science Foundation of China (21274131, 51203139, 21161009), Natural Science Foundation of Jiangxi Province (20132BAB203023 and 20132BAB203004), Science and Technology Plan Projects of Jiangxi Provincial Education Department (GJJ13723), Excellent Doctoral Cultivation Fund of New Materials and Process Engineering Top Key Discipline in Zhejiang Province (G9717101077), China, for financial support.

References

[1] F. Duarte, F.J. Maldonado Hódar, A.F. Pérez Cadenas, L.M. Madeira, Fenton-like degradation of azo-dye Orange II catalyzed by transition metals on carbon aerogels, Appl. Catal., B 85 (2009) 139–147.
[2] C. Flox, S. Ammar, C. Arias, E. Brillas, A.V. Vargas-Zavala, R. Abdelhedi, Electro-Fenton and photoelectro-Fenton degradation of indigo carmine in acidic aqueous medium, Appl. Catal., B 67 (2006) 93–104.
[3] Y. Satyawali, M. Balakrishnan, Wastewater treatment in molasses-based alcohol distilleries for COD and color removal: A review, J. Environ. Manage. 86 (2008) 481–497.
[4] F. EI-Gohary, A. Tawfik, Decolorization and COD reduction of disperse and reactive dyes wastewater using chemical-coagulation followed by sequential batch reactor (SBR) process, Desalination 249 (2009) 1159–1164.
[5] M.C. Yeber, J. Rodríguez, J. Freer, J. Baeza, N. Durán, H.D. Mansilla, Advanced oxidation of a pulp mill bleaching wastewater, Chemosphere 39 (1999) 1679–1688.
[6] C.C. Zhan, F. Chen, H.H. Dai, J.T. Yang, M.Q. Zhong, Photocatalytic activity of sulfated Mo-doped TiO_2@-fumed SiO_2 composite: A mesoporous structure for methyl orange degradation, Chem. Eng. J. 225 (2013) 695–703.
[7] Y.Z. Wang, M.Q Zhong, F. Chen, J.T. Yang, Visible light photocatalytic activity of TiO_2/D-PVA for MO degradation, Appl. Catal., B 90 (2009) 249–254
[8] J.M. Poyatos, M.M. Muñio, M.C. Almecija, J.C. Torres, E. Hontoria, F. Osorio, Advanced oxidation processes for wastewater treatment: State of the art, Water Air Soil Pollut. 205 (2010) 187–204.
[9] T.M. Elmorsi, Y.M. Riyad, Z.H. Mohamed, H.M.H. Abd El Bary, Decolorization of mordant red 73 azo dye in water using H_2O_2/UV and photo-Fenton treatment, J. Hazard. Mater. 174 (2010) 352–358.
[10] F.H. AlHamedi, M.A. Rauf, S.S. Ashraf, Degradation studies of Rhodamine B in the presence of UV/H_2O_2, Desalination 239 (2009) 159–166.
[11] S.G. Schrank, J.N.R. dos Santos, D.S. Souza, E.E.S. Souza, Decolourisation effects of Vat Green 01 textile dye and textile wastewater using H_2O_2/UV process, J. Photochem. Photobiol., A 186 (2007) 125–129.
[12] M. Neamtu, I. Siminiceanu, A. Yediler, A. Kettrup, Kinetics of colourization and mineralization of reactive azo dyes in aqueous solution UV/H_2O_2 oxidation, Dyes Pigm. 53 (2002) 93–99.
[13] A. Ariapad, M.A. Zanjanchi, Effect of successive incorporation of tungstophosphoric acid into TiO_2 on the activity of photocatalysts for the degradation of methylene blue, Superlattices Microstruct. 49 (2011) 422–432.
[14] N.M. Mahmoodi, M. Arami, N.Y. Limaee, N.S. Tabrizi, Decolorization and aromatic ring degradation kinetics of direct red 80 by UV oxidation in the presence of hydrogen peroxide utilizing TiO_2 as a photocatalyst, Chem. Eng. J. 112 (2005) 191–196.
[15] W. Chu, C.C. Wong, The photocatalytic degradation of dicamba in TiO_2 suspensions with the help of hydrogen peroxide by different near UV irradiations, Water Res. 38 (2004) 1037–1043.
[16] S. Kim, H. Park, W. Choi, Comparative study of homogeneous and heterogeneous photocatalytic redox reactions: $PW_{12}O_{40}^{3-}$ vs TiO_2, J. Phys. Chem. B 108 (2004) 6402–6411.
[17] D. Gould, W.P. Griffith, M. Spiro, Polyoxometalate catalysis of dye bleaching by hydrogen peroxide, J. Mol. Catal. A: Chem. 175 (2001) 289–291.
[18] S.R. Mukai, T. Sugiyama, H. Tamon, Immobilization of heteropoly acids in the network structure of carbon gels, Appl. Catal., A 256 (2003) 99–105.
[19] F. Lefebvre, P. Dupont, A. Auroux, Auroux, Study of the acidity of $H_3PW_{12}O_{40}$ supported on activated carbon by microcalorimetry and methanol dehydration reaction, React. Kinet. Catal. Lett. 55 (1995) 3–9.
[20] H.J. Kim, Y.G. Shul, H. Han, Synthesis of heteropoly-acid ($H_3PW_{12}O_{40}$)/SiO_2 nanoparticles and their catalytic properties, Appl. Catal., A 299 (2006) 46–51.

[21] X.H. Mo, E. Lotero, C.Q. Lu, Y.J. Liu, J.G. Goodwin, A novel sulfonated carbon composite solid acid catalyst for biodiesel synthesis, Catal. Lett. 123 (2008) 1–6.
[22] T. Ito, K. Inumaru, M. Misono, Structure of porous aggregates of the ammoniumsalt of dodecatungstophosphoric acid, $(NH_4)_3PW_{12}O_{40}$: Unidirectionally oriented self-assembly of nano-crystallites, J. Phys. Chem. B 101 (1997) 9958–9963.
[23] J. Haber, K. Pamin, L. Matachowski, B. Napruszewska, J. Połtowicz, Potassium and silver salts of tungstophosphoric acid as catalysts in dehydration of ethanol and hydration of ethylene, J. Catal. 207 (2002) 296–306.
[24] C.C. Chen, Q. Wang, P.X. Lei, W.J. Song, W.H. Ma, J.C. Zhao, Photodegradation of dye pollutants catalyzed by porous $K_3PW_{12}O_{40}$ under visible irradiation, Environ. Sci. Technol. 40 (2006) 3965–3970.
[25] C.J. Jiang, Y.H. Guo, C.G. Hu, D.F. Li, Photocatalytic degradation of dye naphthol blue black in the presence of zirconia-supported Ti-substituted Keggin-type polyoxometalates, Mater. Res. Bull. 39 (2004) 25–261.
[26] Y.H. Guo, C.W. Hu, Porous hybrid photocatalysts based on polyoxometalates, J. Cluster Sci. 14 (2003) 505–526.
[27] P. Zhang, C.L. Shao, Z.Y. Zhang, M.Y. Zhang, J.B. Mu, Z.C. Guo, Y.C. Liu, TiO_2@carbon core/shell nanofibers: Controllable preparation and enhanced visible photocatalytic properties, Nanoscale 3 (2011) 2943–2949.
[28] A. Akyol, H.C. Yatmaz, M. Bayramoglu, Photocatalytic decolorization of remazol red RR in aqueous ZnO suspensions, Appl. Catal., B 54 (2004) 19–24.
[29] S.R. Kanel, B. Neppolian, H. Choi, J.W. Yang, Heterogeneous catalytic oxidation of phenanthrene by hydrogen peroxide in soil slurry: Kinetics, mechanism, and implication, Soil Sediment Contam. 12 (2003) 101–117.
[30] J.H. Deng, J.Y. Jiang, Y.Y. Zhang, X.P. Lin, C.M. Du, Y. Xiong, $FeVO_4$ as a highly active heterogeneous Fenton-like catalyst towards the degradation of Orange II, Appl. Catal., B 84 (2008) 468–473.
[31] Z. He, C. Sun, S. Yang, Y. Ding, H. He, Z. Wang, Photocatalytic degradation of rhodamine B by Bi_2WO_6 with electron accepting agent under microwave irradiation: Mechanism and pathway, J. Hazard. Mater. 162 (2009) 1477–1486.
[32] K. Yu, S. Sun, H. He, C. Sun, C. Gu, Y. Ju, Visible light driven photocatalytic degradation of rhodamine B over Na_2BiO_3: Pathways and mechanism, J. Phys. Chem. A 113 (2009) 10024–10032.
[33] A. Mylonas, E. Papaconstantinou, On the mechanism of photocatalytic degradation of chlorinated phenols to CO_2 and HCl by polyoxometalates, J. Photochem. Photobiol., A 94 (1996) 77–82.
[34] G. Moon, Y. Park, W. Kim, W. Choi, Photochemical loading of metal nanoparticles on reduced graphene oxide sheets using phosphotungstate, Carbon 49 (2011) 3454–3462.